Modelling intersite dependence for regional frequency analysis of extreme marine events

Jérôme Weiss, Pietro Bernardara, Michel Benoit

Modelling intersite dependence for regional frequency analysis of extreme marine events

Jérôme Weiss [1,2], Pietro Bernardara [1,3], Michel Benoit [1,2]

[1] Université Paris-Est, Saint-Venant Hydraulics Laboratory (ENPC, EDF R&D, CEREMA), Chatou, France
[2] EDF R&D Laboratoire National d'Hydraulique et Environnement (LNHE), Chatou, France
[3] EDF Energy R&D UK Centre, London, UK

Abstract

The duration of observation at a site of interest is generally too low to reliably estimate marine extremes. Regional frequency analysis (RFA), by exploiting the similarity between sites, can help to reduce uncertainties inherent to local analyses. Extreme observations in a homogeneous region are especially assumed to follow a common regional distribution, up to a local index. The regional pooling method, by gathering observations from different sites into a regional sample, can be employed to estimate the regional distribution. However, such a procedure may be highly affected by intersite dependence in the regional sample. This paper derives a theoretical model of intersite dependence, dedicated to the regional pooling method in a "*peaks over threshold*" framework. This model expresses the tendency of sites to display a similar behavior during a storm generating extreme observations, by describing both the storm propagation in the region and the storm intensity. The proposed model allows the assessment of i) the regional effective duration of the regional sample and ii) different regional hazards, e.g., return periods of storms. An application to the estimation of extreme significant wave heights from the numerical sea-state database ANEMOC-2 is provided, where different patterns of regional dependence are highlighted.

Keywords: regional frequency analysis, pooling, intersite dependence, extremes, significant wave heights

1 Introduction

The design of off-shore structures, or coastal protections preventing shoreline areas from marine flooding, particularly requires an accurate estimation of the probability of occurrence of extreme marine events (e.g., extreme storm surges or wave heights). High return levels can be inferred through a local statistical analysis of extremes, from a time series observed at a given site. However, a potential issue is the local duration of observation, generally too low to accurately estimate return levels of interest. For example, wave records from buoys are usually shorter than 20-30 years.

Regional frequency analysis (RFA) can help to reduce these uncertainties, by exploiting the information shared by similar sites in a region. When based on the index-flood method [*Dalrymple,* 1960], RFA assumes that extreme observations in a homogeneous region follow a common regional probability distribution, up to a local index representing the local specificities of each site.

A possible approach to estimate the parameters of the regional distribution is the regional pooling method [*Bernardara et al.,* 2011]. The principle is to pool the data normalized by the local index in a single regional sample, the latter being used to fit the regional distribution. This method is also referred to as the station-year method [*Buishand*, 1991] and illustrates the principle of "*trading space for time*". However, it assumes intersite independence [*Cunnane*, 1988; *Madsen and Rosbjerg*, 1997; *Stewart et al.*, 1999], which cannot be deemed realistic: indeed, for example, a storm is likely to generate dependent extremes at different sites. Thus, *Dales and Reed* [1989] and *Stewart et al.* [1999] questioned the relevance of regional pooling when intersite dependence is ignored, and showed its approximate nature. Intersite dependence in regional pooling is actually closely related to the concept of regional effective duration [*Bernardara et al.*, 2011].

87 The regional effective duration, denoted by D_{eff}, can be defined as the effective
88 duration of observation of the regional sample filtered of any intersite dependence. For
89 example, if the times series recorded in different sites from a given region are considered
90 independent, pooling data from 10 sites, each having 30 years of observation, is equivalent to
91 sample 300 years of "effective duration". This is not the case in the presence of intersite
92 dependence. At the same time, the highest independent normalized observation in the region
93 is viewed as the largest in D_{eff} years of record. It can be used to both reflect the relevance of
94 RFA to a local analysis and to estimate empirical regional return periods. However,
95 *Kergadallan* [2013] pointed out that one limitation of RFA is the difficulty to evaluate D_{eff}.
96 As an illustration, most of regional pooling studies are based on a simplifying hypothesis. For
97 example, *Hjalimarsom and Thomas* [1992], *Bernardara et al.* [2011] and *Bardet et al.* [2011]
98 assumed D_{eff} as the sum of all the local durations, hence assuming intersite independency.
99 *Dalrymple* [1958] expressed that records cannot be expanded to yield an effective duration
100 equal to the sum of local durations. In this work, it is conversely assumed that D_{eff} can be
101 formulated as the typical local duration, implicitly considering perfect intersite dependence.
102 The actual value is likely to lie between these two extreme cases. A realistic estimation of D_{eff}
103 requires a proper characterization of intersite dependence.
104 A consequence of intersite dependence is a loss of information [*Reed*, 1994]. For
105 example, when a storm impacts several sites, there is redundancy of information because
106 observed extremes stem from the same meteorological event. Several studies assessed the
107 effects of intersite dependence in the framework of RFA. For example, the effective size of
108 samples is reduced [*Bayazit and Önöz*, 2004; *Buishand*, 1991; *Kjeldsen and Rosbjerg*, 2002;
109 *Madsen and Rosbjerg*, 1997; *Rosbjerg and Madsen*, 1996]. *Castellarin et al.* [2008] also
110 observed a decrease of the power of the homogeneity test proposed by *Hosking and Wallis*
111 [1993]. *Stedinger* [1983], *Hosking and Wallis* [1988] and *Rosbjerg and Madsen* [1996]

showed that ignoring intersite dependence in RFA leads to an underestimation of the variance of return levels estimates. When at-site distributions are the main interest, *Smith* [1990] suggests to initially ignore intersite dependence and then correcting a posteriori the regional variance.

A simple way to take into account intersite dependence is to remove it. Some authors proposed its filtering through a spatial declustering procedure, where events impacting several sites are counted only once. To estimate extreme surges with RFA, *Bernardara et al.* [2011] and *Bardet et al.* [2011] formed the regional sample with the highest observations among extremes occurring within 72 hours in the study area. However, the major disadvantage of such an approach is a significant loss of information on the spatial dynamics of extremes generated by a single storm. Moreover, this approach does not introduce any technique to estimate D_{eff}.

Intersite dependence can also be modeled. *Cooley et al.* [2012] and *Bernard et al.* [2013] deplored the lack of an explicit modeling of intersite dependence for RFA. Nevertheless, *Renard and Lang* [2007] and *Renard* [2011] represented the dependence of extreme rainfalls at different sites with elliptical copulas. Extremes at two different sites were also regionally modeled by *Buishand* [1984], through bivariate extreme value theory. An alternative approach, dedicated to annual maxima, was proposed by *Dales and Reed* [1989]; it links distributions of the regional maximum and the typical regional data through an effective number of independent sites.

Most of the papers cited above analyzed series of annual maxima. Yet, an alternative way is to consider exceedances over a high threshold with the "*peaks over threshold*" (POT) method [*Davison and Smith*, 1990]. Its superiority over methods based on annual maxima, for both local and regional estimation of extremes, was demonstrated by *Madsen et al.* [1997a], *Madsen et al.* [1997b] and *Arns et al.* [2013]. Besides, the POT framework is more physically

appealing to handle intersite dependence. For annual maxima, this one is characterized on a yearly basis, and may thus be difficult to interpret: for example, series of annual maxima observed at two distinct sites can be highly statistically correlated, without necessarily being caused by the same meteorological phenomena. Conversely, the POT framework allows reasoning at the scale of the physical event, provided that the concurrence of observations at different sites can be carefully defined [*Mikkelsen et al.*, 1996; *Stewart et al.*, 1999]. In particular, storms generating extreme observations offer an intuitive framework to deal with intersite dependence in a POT approach. *Weiss et al.* [2014] characterized storms through the gathering of extremes neighbors in space and time, and described a procedure to detect them in the context of marine extremes. These storms allow to naturally define the concurrence of observations at the scale of the physical event.

Thus, very few studies addressed the issue of intersite dependence for RFA in a POT framework. *Roth et al.* [2012] used the model of *Dales and Reed* [1989] by grouping POT data into seasonal blocks. It can be argued, that defining the concurrence of observations through a wide temporal block (the season) may result in a loss of information on both the spatial coverage and the intensity of the physical events generating extremes. *Mikkelsen et al.* [1996], *Rosbjerg and Madsen* [1996], *Madsen and Rosbjerg* [1998] and *Madsen et al.* [2002] proposed regional regression models, which are not based on the index-flood procedure used in this paper. Similar to geostatistics, their models explicitly account for intersite correlation, where the concurrence of observations is defined through the overlap of POT data in a short time window. *Madsen and Rosbjerg* [1997] corrected the variance of the regional distribution parameters with an effective number of independent sites, based on a regional average correlation coefficient. However, in the latter references, although the concurrence of observations is defined in a physically appealing way, only the pairwise dependence is modeled. Moving towards a more global model of intersite dependence indicating, for

example, the tendency of sites in a region to behave similarly during a storm, would help to characterize different regional hazards.

The estimation of extreme events by RFA allows to tackle the open question of the difference between regional and local return period. In particular, note that to estimate the return period of a storm affecting a given area, synoptic variables are usually defined first. *Della-Marta and Pinto* [2009] characterized a storm by the minimum central pressure and the maximum vorticity reached during its track; *Pinto et al.* [2012] used the wind speed maximum; a more general spatial index, reflecting both the magnitude and the spatial extent, was defined by *Della-Marta et al.* [2009], who then estimated the return period from these synoptic variables. By construction, such an estimate corresponds to a "regional" return period, namely the return period of a storm which can occur anywhere in the study area. However, for practical applications (e.g., protection design), a local return period must be estimated. For example, it is clear that a storm whose regional return period is 50 years will not generate everywhere in the area wave heights (or storm surges) corresponding to a 50-year return period. In particular, the link between the regional return period of a storm and the return period of a given observed variable generated by the storm at a particular location remains unknown. Note that *Della-Marta et al.* [2009] showed that regional return periods share up to about half of the variability of the local return periods. In this study, we will show how a proper treatment of intersite dependence can help to describe the relation between the regional and the local return period of a storm.

The objective of this paper is to develop a global model of intersite dependence for RFA, specifically dedicated to the regional pooling method and POT data, by reasoning at the storm scale. Distributions of the regional storm maximum and the typical regional storm data are linked through a function of *regional dependence*, describing both the propagation of

storms and their regional intensity. The proposed model allows the derivation of different regional hazards and the regional effective duration.

The model of regional dependence is developed in section 2, including its implications on the regional pooling method (section 2.4). An application to the estimation of extreme significant wave heights from the numerical database ANEMOC-2 is shown in section 3.

2 Methodology

2.1 Extraction of storms

To characterize the intersite dependence, it is first necessary to define the simultaneity of observations in space. If data are sampled every hour, the reference for simultaneity can be, for example, the hourly scale. However, as extreme oceano-meteorological conditions can last from several hours to several days, the temporal dimension should be added to describe the spatial dependence. In this paper, the scale of the physical events generating marine extremes (storms) is taken as the reference to define the simultaneity of observations in space.

A storm is thus directly characterized through the variable of interest (e.g., wave height or storm surge), being defined as a physical event generating marine extremes in at least one site in the study area. In the literature, the tracking of storms often relies on a nearest-neighbor search in space and time [e.g., *Leckebusch et al.*, 2008; *Renggli et al.*, 2010]. A spatio-temporal declustering procedure is thus employed to detect storms and to reflect their propagation in space and time. In particular, extremes neighbors in space and time are supposed to stem from the same storm. The storm extraction algorithm in the context of marine extremes is described in *Weiss et al.* [2014], trying to reproduce at best the physical dynamics of the storms, while taking into account the spatio-temporal resolution of observations. Moreover, a “double-threshold” approach is employed to separate physical considerations from statistical ones [*Bernardara et al.*, 2014].

At a given site, the impact of a storm is characterized by observations exceeding the "physical threshold" q_p, defined as the p-quantile of the initial time series, with p close to 1. In order to get independent data at site scale, only the peak value W_s^i is retained to summarize the storm s at site i (which implies that all other extremes occurring during that storm are discarded).

Only the most intense storm events are now considered for statistical aspects. New thresholds, denoted u and higher than the quantiles q_p, are selected corresponding to the occurrence of λ storms per year on average at each site. In particular, if d_i years of data are available at site i, the $n_i = \lambda d_i$ highest W_s^i are retained to form the n_i-sample X_s^i. The "statistical threshold" u_i, exceeded on average λ times per year, is then defined as the smallest observation from X_s^i (minus an infinitesimal quantity). Storms are then statistically redefined: if site i was impacted by storm s, it is from now on impacted by s if and only if u_i is exceeded.

2.2 Regional frequency analysis

Extreme events are estimated in this paper from exceedances over a high threshold. According to *Pickands* [1975], the Generalized Pareto Distribution (GPD) represents the natural distribution for such exceedances. For ease of notation, the index s denoting the storm is omitted in this section. For site i, let u_i be the storm threshold which is exceeded on average λ times per year. The n_i-sample X^i, denoting the exceedances of u_i, is assumed to be drawn from a GPD: $X^i \sim \mathrm{GPD}(u_i, \alpha_i, k_i)$, where $\alpha_i > 0$ and k_i are, respectively, a scale and a shape parameter. In particular, the p-quantile of X^i is:

$$x_p^i = \begin{cases} u_i - \alpha_i / k_i \left(1 - (1-p)^{-k_i}\right), & k_i \neq 0 \\ u_i - \alpha_i \log(1-p), & k_i = 0 \end{cases} \qquad (1)$$

The right tail of the GPD is bounded when $k_i < 0$, and unbounded when $k_i \geq 0$. The T-year return level, i.e., the value exceeded on average once every T years, is given by $x^i_{1-1/\lambda T}$ [*Rosbjerg*, 1985].

A homogeneity hypothesis is required for RFA based on the index-flood method. Observations from sites coming from a homogeneous region are supposed to follow the same regional probability distribution, up to a local index representing the local specificities of a site. In this paper, homogeneous regions are formed following *Weiss et al.* [2014], where typical storm footprints are identified with a clustering algorithm based on a criterion of storm propagation. In particular, sites from a given region are likely to be impacted by the same storms, and any storm impacting a region is likely to remain enclosed in this region.

For a homogenous region of N sites, let μ_i be the local index of the site $i = 1,\ldots,N$. The normalized variable $Y = X^i / \mu_i$ is supposed to be independent of i, with cumulative distribution function (c.d.f.) F_r. *Roth et al.* [2012] showed that dealing with exceedances over a high threshold necessarily implies that the local index has to be a multiple of this threshold. Here, as in *Roth et al.* [2012] and *Weiss et al.* [2014], μ_i is therefore chosen as the threshold u_i. This implies that $Y \sim \text{GPD}(1, \gamma, k)$, where: i) the regional scale parameter satisfies $\gamma = \alpha_i / u_i$ and ii) the shape parameter $k_i = k$ is constant over the region. From these relationships, $X^i \sim \text{GPD}(u_i, \gamma u_i, k)$. For site i, the T-year return level is obtained by multiplying the regional T-year return level by the local index: $x^i_{1-1/\lambda T} = u_i y_{1-1/\lambda T}$.

The two regional parameters (γ, k) can be estimated with the regional pooling method. However, as sites in a region are likely to be impacted by the same storms, a strong intersite dependence is expected. If ignored, this may affect the estimation process. Thus, this dependence is firstly modeled as outlined in section 2.3, before the regional pooling method is described in section 2.4.

2.3 Modeling of regional dependence

2.3.1 Notations

Let λ_r be the mean annual number of storms in the region and Z_s^i the Bernoulli variable which is 1 if storm *s* impacts site *i* and 0 otherwise. When storm *s* impacts site *i*, the observed normalized extreme with c.d.f. F_r is denoted by $Y_s^i = X_s^i / u_i$. Note that $Y_s^i \geq 1$. The storm *s* can be summarized in the region by the multivariate random variable $\eta_s = (\eta_s^1,...,\eta_s^N)$, where $\eta_s^i = Y_s^i Z_s^i$. The storm regional maximum is then defined as $M_s = \max_{i=1,..,N} \eta_s^i$. As at least one site is impacted by the storm *s*, $M_s \geq 1$.

2.3.2 Distribution of the storm regional maximum

First, note that due to the statistical redefinition of storms at the end of section 2.1, Z_s^i takes the value 1 with probability λ / λ_r, independently of *i*. Moreover, by the regional homogeneity hypothesis from section 2.2, the distribution of η_s^i does not depend on *i*:

$$\forall x \geq 1,\ P(\eta_s^i > x) = P(Z_s^i = 1) P(\eta_s^i > x \mid Z_s^i = 1) = \frac{\lambda}{\lambda_r}(1 - F_r(x)) \tag{2}$$

For $x \geq 1$, the distribution of M_s can be obtained through the following decomposition:

$$P(M_s > x) = P(\max_{i=1,..,N} \eta_s^i > x) = \sum_{i=1}^{N-1} P(\eta_s^i > x,\ \max_{j=i+1,..,N} \eta_s^j \leq x) + P(\eta_s^N > x) \tag{3}$$

Now, as the distribution of η_s^i is independent of *i*:

$$P(M_s > x) = P(\eta_s^1 > x)[1 + \sum_{i=1}^{N-1} P(\max_{j=i+1,..,N} \eta_s^j \leq x \mid \eta_s^i > x)] \tag{4}$$

From (2), this leads to:

$$P(M_s > x) = P(\eta_s^1 > x)\varphi(x) = (1 - F_r(x))\frac{\lambda}{\lambda_r}\varphi(x) \tag{5}$$

where

$$\varphi(x) = 1 + \sum_{i=1}^{N-1} P\left(\max_{j=i+1,..,N} \eta_s^j \leq x \mid \eta_s^i > x\right),\ x \geq 1 \qquad (6)$$

The distribution of M_s can be thus written in terms of the regional distribution F_r and φ.

2.3.3 Characterization of the regional dependence

The function φ reflects the regional dependence. Situations of independence and perfect dependence, illustrating extreme cases of dependence, can be reinterpreted through equation (6) with $x = 1$. In particular, the region is *regional-independent* ($r - \perp\!\!\!\perp$) if and only if $\varphi \equiv N$; in that case, a storm impacts only one site in the region, whatever its intensity. Conversely, the region is *perfectly regional-dependent* ($p-rd$) if and only if $\varphi \equiv 1$; a storm impacts every site in the region and, whatever its intensity, the generated (normalized) extremes vary the same way. Between these two extremal situations, φ takes values between 1 and N.

By construction, φ relates both the storm propagation in the region and the storm intensity. It expresses the tendency of sites to display a similar behavior during a storm. The regional dependence is stronger when φ is small, hence indicating that most of the sites are impacted by a storm, and are likely to react the same way in terms of normalized extremes.

φ is influenced by the number N of sites in the region. In order to compare φ between different regions, the effect of N can be removed through the following adimensional function:

$$\Phi(x) = \frac{N - \varphi(x)}{N - 1},\ x \geq 1 \qquad (7)$$

where Φ, lying between 0 and 1, is near to 1 when regional dependence is strong.

2.3.4 Assessment of regional hazards

A regional hazard is an event occurring at the regional scale, whose probabilistic description is related to collective risk assessment. The following examples of regional hazards are expressed in terms of the function of regional dependence φ.

A first example is the mean number $\beta_s(x)$ of impacted sites with normalized intensity larger than $x \geq 1$ when the storm regional maximum is larger than x:

$$\beta_s(x) = E[\sum_{i=1}^{N} 1_{\eta_s^i > x \,|\, M_s > x}] \tag{8}$$

From equation (5):

$$\beta_s(x) = NP(\eta_s^1 > x \,|\, M_s > x) = N\frac{P(\eta_s^1 > x)}{P(M_s > x)} = \frac{N}{\varphi(x)} \tag{9}$$

In particular, the mean number of impacted sites during any storm is given by $\beta_s(1) = N / \varphi(1)$. Note that this is coherent with the definitions of *regional-independence* and *perfect regional-dependence*.

Another example is the evaluation of the regional return period of a particular storm, and how it is related to its local return period. Let s be a given storm, and denote by $x \geq 1$ its corresponding normalized intensity. The *regional return period* of s, T_r, is defined as the average time between storms impacting *at least one site* in the region with a normalized intensity greater than x, i.e.:

$$T_r = \frac{1}{\lambda_r P(M_s > x)} \tag{10}$$

The *local return period* of s, T, is defined as the average time between storms impacting *a given site* in the region with a normalized intensity greater than x:

$$T = \frac{1}{\lambda(1 - F_r(x))} \tag{11}$$

From (5), T_r and T are related through:

$$T_r = \frac{T}{\varphi(x)} \quad (12)$$

2.4 Regional pooling method

2.4.1 Construction of the regional sample

The regional pooling method is used to estimate the regional distribution F_r. However, due to the presence of intersite dependence, events impacting several sites must be counted only once. Storms presented in section 2.1 are a convenient way to filter intersite dependence, as each storm describes the regional footprint of a particular event generating extremes.

In particular, the distribution of the storm regional maximum M_s is now assumed to be the same as the regional distribution F_r. This assumption was implicitly made in *Bernardara et al.* [2011] and *Bardet et al.* [2011], where the regional distribution was estimated from the highest normalized surges occurred within 72 hours in the region. In other words, the distribution of the maximum of a regional cluster is identical to the distribution of a generic element of this cluster. The same assumption is often made in a POT time series framework, as explained by Anderson in the discussion of the paper by *Davison and Smith* [1990]: "*this apparent paradox is a consequence of length-biased sampling: a randomly chosen exceedance has a disproportionate chance of coming from a large cluster, and in large clusters there tend to be large excesses.*" However, in practice, the validity of this assumption must be verified. For example, the two-sample Anderson-Darling test [*Scholz and Stephens,* 1987] can be performed at each site *i* to evaluate the null hypothesis that Y_s^i and M_s have the same distribution.

If n_r independent storms are observed in the region, the regional sample is thus formed by the n_r-sample of storm regional maxima M_s, and corresponds to D_{eff} years of regional effective duration.

The assumption that the storm regional maximum M_s is the same as the regional distribution F_r depends on the data at hand. When this hypothesis is not verified, the following alternative strategies nevertheless allow to perform a RFA:

i) Remove sites of which Anderson-Darling p-values are too low (for example, lower than 0.01) to accept this hypothesis. The application of the model of regional dependence and the estimation of F_r can then be performed on the remaining sites.

ii) Form the regional sample with random (normalized) observations from each storm, instead of using the storm regional maxima M_s. F_r can still be estimated by pooling, directly from this new regional sample. However, the simplified model of dependence (section 2.4.3) is not valid anymore, as φ is not a constant function. It would be possible to update equation (14) by letting the regional effective duration depend on regional quantiles.

iii) Use another method to perform the RFA, e.g., the regional L-moments method of *Hosking and Wallis* [1997]. The model of regional dependence developed in this paper, dedicated to the pooling method, does not apply anymore in this case.

2.4.2 Estimation of the regional distribution F_r.

The two regional parameters (γ, k), see section 2.2, are estimated from the regional sample. Penalized maximum likelihood estimation (PMLE) [*Coles and Dixon*, 1999] is used in this study. The principle is to combine the efficiency of maximum likelihood estimators for large sample sizes and the reliability of the probability weighted moment estimators for small sample sizes. In particular, high estimates of the shape parameter k are penalized. PMLE is implemented in the function fitgpd of the POT package [*Ribatet*, 2007], in the statistical computing environment R (R Development Core Team, 2013). Uncertainties on estimates of (γ, k) are here assessed with a bootstrap procedure: 10,000 replications of the (γ, k) values are obtained with PMLE from resamples of the regional sample.

353 *2.4.3 Simplification of the model of regional dependence*

354 The regional pooling method presented in this paper assumes that the distribution of
355 the storm regional maximum M_s is the same as the regional distribution F_r. The model of
356 regional dependence in section 2.3 can thus be simplified. Indeed, from (5), this assumption
357 implies that φ becomes a constant function:

$$\forall x \geq 1,\ P(M_s > x) = 1 - F_r(x) \leftrightarrow \varphi(x) = \frac{\lambda_r}{\lambda} \qquad (13)$$

358 As φ is constant, the way sites react during a storm does not depend on the intensity of the
359 storm. Similarly, *Dales and Reed* [1989] applied their model to rainfall annual maxima and
360 observed that the effective number of sites, summarizing the spatial dependence, did not seem
361 to depend on a particular regional intensity.

362 *2.4.4 The regional effective duration D_{eff}*

363 The pooling procedure yields D_{eff} years of regional effective duration. D_{eff} is closely
364 related to the degree of regional dependence; in particular, D_{eff} is expected to be low when
365 regional dependence is strong.

366 First, the two simplistic situations of regional dependence (section 2.3.3) are
367 considered. Let $\bar{d} = \sum d_i / N$ be the mean local duration, where d_i is the local duration of
368 observation at site i and N is the number of sites in the region. If the region is $r-1$, a storm
369 impacts only one site in the region. In that case, each observation from any site brings new
370 information, and D_{eff} can be written as the sum of all the local durations: $D_{eff} = N\bar{d}$.
371 Conversely, if the region is $p-rd$, a storm impacts every site in the region. Here, the typical
372 local duration of one site constitutes D_{eff}, as the information from other sites is purely
373 redundant. This can be reflected by taking, for example, D_{eff} as the mean local duration: $D_{eff} =$
374 $\bar{d}$. It is now assumed that, between these two extremal cases, D_{eff} can be more realistically
375 expressed by:

$$D_{eff} = \varphi \bar{d} \quad (14)$$

where φ, lying between 1 and N, is the degree of regional dependence. Note that the situations of $p-rd$ and $r-$ are respectively obtained for $\varphi = 1$ and $\varphi = N$. From equation (13), stating that $\varphi = \lambda_r / \lambda$, its theoretical value is $D_{eff} = \lambda_r \bar{d} / \lambda$.

The mean annual number of storms in the region λ_r can be naturally estimated by $n_r / \bar{d}$, where n_r is the number of observed storms. An estimate of D_{eff} is then:

$$\hat{D}_{eff} = \frac{n_r}{\lambda} \quad (15)$$

Let $n_{r,t}$ be the number of observed storms during year $t = t_1,\ldots,t_\tau$ in the region, where t_1 and t_τ indicate the first and the last year of observation in the region, respectively. The overall number of observed storms n_r is obtained by summing the $n_{r,t}$ for $t = t_1,\ldots,t_\tau$. By assuming that the $n_{r,t}$ are independent and identically distributed with common mean λ_r and standard deviation σ_r, the central limit theorem followed by the Slutsky's lemma allow to derive new confidence intervals for D_{eff}:

$$[\hat{D}_{eff} - z_{1-\alpha/2} \frac{\hat{\sigma}_r \sqrt{\tau}}{\lambda}, \hat{D}_{eff} + z_{1-\alpha/2} \frac{\hat{\sigma}_r \sqrt{\tau}}{\lambda}] \quad (16)$$

where $z_{1-\alpha/2}$ is the quantile of order $1-\alpha/2$ of the standard normal distribution, $\hat{\sigma}_r$ is the empirical standard deviation of the $n_{r,t,}$ and τ is the number of years of observation in the region.

Note that (15) can be used even if periods of observations are different, and in the presence of missing data. This formula also guarantees that $\hat{D}_{eff} \geq \max_{i=1,..,N} d_i$, coherently with what might be expected from the regional effective duration. Besides, it reflects the importance to extract storms such that their mean annual occurrence λ at the local scale is common to all sites.

As F_r is estimated from D_{eff} years of pooled data, the underlying principle is that any site in the region can be indifferently impacted by a given storm. Parenthetically, with no preferential storm track in the region, the regional pooling method is coherent with the identification of storms footprints to form homogeneous regions. In particular, the regional sample illustrates that, for a generic site, λ storms per year, on average, were observed during D_{eff} years. D_{eff} thus helps to reflect the relevance of RFA to a local analysis. Indeed, pooling enables to estimate extreme events at site i from D_{eff} years of data, compared to d_i years for a local analysis.

2.4.5 Evaluation of storm return periods

The regional pooling method allows to distinguish between local and regional return periods of normalized storm events (see section 2.3.4 for the corresponding definitions), both at the empirical and theoretical levels. Let s be a given storm from the regional sample, and denote by x its corresponding normalized intensity.

Using the Weibull plotting position, its empirical local return period $\tilde{T}_{s,loc}$ is:

$$\tilde{T}_{s,loc} = \frac{D_{eff} + 1}{n_r + 1 - \text{rank}(s)} \tag{17}$$

where rank(s) denotes the rank of s in the regional sample. For example, if s is the most intense storm observed in the regional sample, then $\tilde{T}_{s,loc}$ is about D_{eff} years. Besides, the theoretical local return period $\overline{T}_{s,loc}$ of s is given by equation (11). We recall that $\overline{T}_{s,loc}$ corresponds to the theoretical return period of storm s at site scale (i.e., at any site of the region). Using (12) and (13), the theoretical regional return period $\overline{T}_{s,reg}$ is given by:

$$\overline{T}_{s,reg} = \frac{\lambda}{\lambda_r}\overline{T}_{s,loc} \tag{18}$$

The empirical regional return period $\tilde{T}_{s,reg}$ is linked with $\tilde{T}_{s,loc}$ through a similar relation.

3 Application

3.1 Data used

ANEMOC-2 (Atlas Numérique d'États de Mer Océaniques et Côtiers - Numerical Atlas of Oceanic and Coastal Sea states) is a numerical sea-state hindcast database covering the Atlantic Ocean over the period 1979-2009 (31 years). It has been developed at Saint-Venant Laboratory for Hydraulics and EDF R&D LNHE [*Laugel*, 2013]. The simulations of wave conditions have been carried out with the third-generation spectral wave model TOMAWAC [*Benoit et al.*, 1996] forced by wind fields from the CFSR reanalysis database [*Saha et al.*, 2010].

The spatial resolution of the so-called "oceanic mesh" of ANEMOC-2 ranges from about 120 km over the Northern part of the Atlantic Ocean down to about 20 km along the European coast and 10 km along the French coast. Note this grid is supplemented by a "coastal mesh" whose resolution is finer on the continental shelf, in the Channel and along the French coast. For the present study, however, only data from the oceanic mesh is used, and only a subset of 1847 nodes amongst the 13426 nodes of the full oceanic mesh is selected, at locations plotted in Figure 1.

Among the wave parameters available with an hourly resolution in ANEMOC-2, we consider here the significant wave height, denoted H_s, which is usually the preferred parameter to summarize sea state intensity. TOMAWAC computes this wave height from the zero-order moment of the wave spectrum. Hourly series of significant wave heights H_s over the period 1979-2009 are thus extracted for the 1847 selected sites. The objective here is to apply the proposed methodology i) to characterize the regional dependence over this area and ii) to estimate extreme H_s by the regional pooling method.

438 3.2 Preparation of data for RFA

439 More details for this section may be found in *Weiss et al.* [2014], where the same
440 dataset was used.

441 The physical extraction of storms generating extreme H_s, described in the beginning of
442 section 2.1 with $p = 0.995$, leads to 5939 storms. *Weiss et al.* [2014] performed a sensitivity
443 analysis and found that storms are properly detected when $p = 0.995$. A quick analysis reveals
444 that, on average: i) there are 192 storms per year in the study area, ii) a storm impacts 38 sites
445 and iii) a storm lasts 12.5 hours at site scale. These storms serve to form physically
446 homogeneous regions, by detecting the most typical storms footprints in the study area. The
447 footprints of the storms of 15-18 February 1986, 11-13 December 1990 and 23-24 January
448 2009 (Klaus) are shown in Figure 2.

449 Storms are then statistically redefined, following the methodology presented in section
450 2.1. In particular, $\lambda = 1$ storm per year are now observed, on average, at each site; 1340 storms
451 are thus retained among the 5939 initial ones. Site *i* is therefore characterized by the sample
452 of H_s over the threshold u_i exceeded on average once per year; the sample size is 31, as 31
453 years of data are available. These thresholds, represented in Figure 3, are also the local indices
454 used for RFA (section 2.2). These storms serve to i) check the statistical homogeneity of the
455 physically homogeneous regions, ii) deal with regional dependence and iii) estimate extreme
456 events with the regional pooling method.

457 RFA can thus be performed on each of the six homogeneous regions delineated in
458 *Weiss et al.* [2014], see Figure 4.

459 3.3 Regional pooling method

460 For each of the six regions, the regional sample is constructed by pooling the observed
461 normalized storm regional maxima, following section 2.4.1. To check whether the storm
462 regional maxima are sampled from the regional distribution F_r, the two-sample Anderson-

463 Darling test is performed. The p-values for the null hypothesis that Y_s^i and M_s have the same
464 distribution, for each site *i* from a given region, are higher than 0.01 for 95% of all sites.
465 Therefore, it may be reasonably assumed that i) the model of regional dependence can be
466 simplified and ii) F_r can be estimated from the regional sample.

467 *3.3.1 Measures of regional dependence*

468 For each region, Table 1 provides some measures of regional dependence defined in
469 sections 2.3.3, 2.3.4 and 2.4.4. Note that there are no missing values in ANEMOC-2 data, and
470 periods of observations are the same for all sites (with a common local duration of d = 31
471 years).

472 Storms are, respectively, most and least most frequent in regions 2 and 6, with 25.2
473 and 2.7 storms per year on average. This is explained here by their size: regions 2 and 6 are,
474 respectively, the largest and the smallest in terms of the number of sites. To compare the
475 degree of regional dependence between regions, this size effect can be removed through the
476 adimensional function Φ defined in equation (7). The regional dependence is thus the
477 strongest in region 5, meaning that sites in this region tend to behave highly similarly during a
478 storm: a large proportion of them are impacted, and the normalized extremes are likely to vary
479 the same way. Conversely, the regional dependence is the weakest in region 2. This can be
480 precised by considering the mean number $\beta_s(1)$ of impacted sites during a storm, see equation
481 (9). Indeed, on average, a storm in region 2 only impacts 18.9 sites (4% of the region),
482 whereas a storm in region 5 impacts 56.6 sites (24% of the region).

483 The regional effective duration D_{eff} and its corresponding 95% confidence interval are
484 estimated following equations (15) and (16). For example, pooling data from the 234 sites of
485 region 5 enables to get a regional sample with D_{eff} = 128 years of independent observations.
486 Note that taking into account the regional dependence considerably reduces what would be
487 obtained under the assumption of intersite independence (in that case, $D_{eff} = Nd$ = 7254 years).

488 Figure 5 shows the evolution of the regional return period T_r against the local return
489 period T for each region, see equation (12). Note that curves for regions 3 and 4 are very close
490 to each other, giving the impression of being superimposed. The simplified model of regional
491 dependence implies that T_r and T are linearly related. For fixed T, T_r is, respectively, the
492 lowest and the highest in regions 2 and 6. For example, Table 1 gives 100_r, i.e., T_r
493 corresponding to T = 100 years. 100_r = 3.964 years in region 2: about every four years on
494 average, a storm in this region causes at least one local 100-year event. Besides, although
495 region 1 is much larger that region 3, note that their 100_r estimates are similar (about 10
496 years). If intersite dependence was assumed, then this quantity would have been, in
497 proportion, much higher in region 3 than in region 1. However, the compensation is due to a
498 stronger regional dependence in region 1. Thus, modeling the regional dependence allows a
499 more realistic assessment of regional hazards.

500 *3.3.2 Estimation of extreme H_s*

501 For each of the six homogeneous regions, the regional GPD parameters (γ, k) are
502 estimated following the procedure outlined in section 2.4.2. These quantities are given in
503 Table 2, as well as the 100-year regional return level $y_{0.99}$. The shape parameter k is positive
504 (corresponding to an unbounded GPD) in regions 1, 4 and 6, suggesting a higher intensity of
505 extreme H_s. The return level plots for each of the six regional distributions, together with the
506 95% confidence intervals obtained by bootstrap, are given in Figure 6. Note that the plotting
507 position depending on the regional effective duration (equation (17)) is used to represent
508 observations from the regional sample, hence allowing the estimation of empirical return
509 periods (see section 3.3.3 for an application to the most intense storms observed).
510 At-site return levels are obtained by multiplying regional return levels by the local
511 indices. Figure 7 shows the map of the estimated at-site 100-year H_s. Estimates for coastal
512 areas are not shown because, as mentioned in section 3.1, the present analysis uses data from

513 the oceanic model of ANEMOC-2, whose resolution is not sufficient for these coastal areas
514 and which includes only parts of the shallow-water effects. In a follow-up of this study, data
515 from the coastal model may improve the simulated sea states in coastal areas. One can note on
516 Figure 7 that 100-year H_s estimates display a coherent spatial pattern, with lower values near
517 the West European coasts. The highest return levels are obtained for sites located in the north-
518 central part of the study area (up to 29.65 m). Note that these estimates are comparable to
519 those from *Caires and Sterl* [2005] and *Weiss et al.* [2014].

520 Compared to a local statistical analysis, the regional pooling method can help to
521 reduce uncertainties in the estimation of extreme events, at a given site. Indeed, extrapolations
522 from a local analysis would be based here on d = 31 years of observations; the regional
523 pooling makes available $D_{eff} > d$ years of data for any site.

524 *3.3.3 Return periods of the most intense storms observed*

525 From the numeric database ANEMOC-2, storms with the highest normalized intensity
526 were observed on February 1986, February 1979, December 1990, February 1988, December
527 1989 and January 2009, respectively in region 1, 2, 3, 4, 5 and 6. Figure 2 displays these
528 storms which occurred in regions 1, 3 and 6.

529 As an application of section 2.4.5, return periods of these storms are provided in Table
530 3, both at the local and regional scales (empirical and theoretical). For example, in region 3,
531 the empirical local return period $\tilde{T}_{s,loc}$ of the storm of 11-13 December 1990 is estimated at
532 280 years. Its theoretical counterpart is quite close ($\bar{T}_{s,loc}$ = 367 years), as indicated by the
533 return level plot for this region (Figure 6). As such a storm was observed only once in 31
534 years of observations in this region, its empirical regional return period $\tilde{T}_{s,reg}$ is logically
535 estimated at 31 years. From equation (18), the model of regional dependence predicts a
536 theoretical regional return period $\bar{T}_{s,reg}$ of 41 years.

4 Conclusions

By exploiting the information shared by statistically similar sites, regional frequency analysis (RFA) can reduce uncertainties in the estimations of high return levels, when at-site durations of observations are short. It is assumed that, in a homogeneous region, extreme observations follow a common regional probability distribution, up to a local index representing the local specificities of a site.

The method of regional pooling is employed in this paper, where normalized observations from different sites are gathered into a regional sample to estimate the regional distribution. In particular, this pooling procedure allows to define D_{eff} years of regional effective duration. D_{eff} is actually closely related to the degree of intersite dependence: for example, D_{eff} is expected to be low when the dependence is strong. Intersite independence is a usual assumption in the literature and practice, although unrealistic: a storm is likely to generate dependent extremes at different sites. We have therefore proposed a theoretical frame to model intersite dependence for the regional pooling method.

Storms are here identified by detecting physical events generating extremes in at least one site in the study area; their spatio-temporal propagation is taken into account through the gathering of extremes neighbors in space and time. Storms allow to naturally define the concurrence of observations at the scale of the physical event, hence enabling to perform a RFA within a "*peaks over threshold*" framework. These storms represent a convenient way to describe regional dependence. In particular, they are the basis to i) construct the regional sample, by filtering the redundancy of information and ii) model the regional dependence.

The distribution of the storm regional maximum is linked to the regional distribution through a function of regional dependence. This function, describing both the storm propagation in the region and the storm intensity, expresses the tendency of sites to display a similar behavior during a storm. The proposed model allows i) a proper evaluation of D_{eff} and

ii) the assessment of different regional hazards: for example, the mean number of impacted sites during a storm, or return periods of storms both at the local and regional scales can be theoretically derived.

An application to significant wave heights from the numerical sea-state database ANEMOC-2 has been provided to demonstrate the capabilities of the model. Six homogeneous regions, corresponding to the most typical storms footprints were delineated in the North-East part of the Atlantic Ocean. Different patterns of regional dependence have been characterized in this area, before applying the regional pooling method to estimate extreme significant wave heights.

Although the proposed example considers significant wave heights, the method can easily be applied to other marine variables. Indeed, it is variable-oriented, in the sense that storms are specifically defined through to the variable of interest only. Moreover, D_{eff} can also be estimated when periods of observations are not the same for all sites, and/or in the presence of missing values. Future works could, for example, apply the proposed model to other marine hazards (e.g., storm surges) to compare how regional dependence manifests compared to significant wave heights.

5 Acknowledgments

The permission to publish the results of this ongoing research study was granted by the Electricité de France (EDF) company. The results in this paper should, of course, be considered as R&D exercises without any significance or embedded commitments upon the real behavior of the EDF power facilities or its regulatory control and licensing. The authors would like to thank Amélie Laugel who kindly provided the ANEMOC-2 data used in this study, and the three anonymous reviewers who improved this paper by their constructive comments and suggestions. The wave data set used for the analyses presented in this article

has been extracted from the ANEMOC-2 database. This dataset can be obtained by request addressed to the corresponding author. The use of this data is restricted to research purpose, all industrial or commercial applications being excluded.

6 References

Arns, A., Wahl, T., Haigh, I. D., Jensen, J. and C. Pattiaratchi (2013), Estimating extreme water level probabilities: A comparison of the direct methods and recommendations for best practice, *Coastal Engineering*, 81, 51-66.

Bardet, L., C.-M. Duluc, V. Rebour and J. L'Her (2011), Regional frequency analysis of extreme storm surges along the French coast, *Natural Hazards and Earth System Sciences*, 11, 6, 1627-1639.

Bayazit M. and B. Önöz (2004), Sampling variances of regional flood quantiles affected by intersitecorrelation, *Journal of Hydrology*, 291, 1–2, 42–51.

Benoit, M., F. Marcos, and F. Becq (1996), Development of a third generation shallow-water wave model with unstructured spatial meshing, in *Proceedings of the 25th International Conference on Coastal Engineering*, pp. 465–478, American Society of Civil Engineers (ASCE), Orlando, Florida.

Bernard, E., Naveau, P., Vrac, M. and O. Mestre (2013), Clustering of maxima: spatial dependencies among heavy rainfall in France, *Journal of Climate*, 26, 7929–7937.

Bernardara, P., Andreewsky M. and M. Benoit (2011), Application of the Regional Frequency Analysis to the estimation of extreme storm surges, *Journal of Geophysical Research*, 116, C02008, 1-11.

Bernardara, P., F. Mazas, X. Kergadallan, and L. Hamm (2014), A two-step framework for over-threshold modelling of environmental extremes, *Nat. Hazards Earth Syst. Sci.*, 14, 635–647.

Buishand, T. A. (1984), Bivariate extreme-value data and the station-year method, *Journal of Hydrology*, 69, 1-4, 77–95.

Buishand, T. A. (1991), Extreme rainfall estimation by combining data from several sites, *Hydrological Sciences*, 36, 4, 345–365.

Caires, S. and A. Sterl (2005), 100-year return value estimates for ocean wind speed and significant wave height from the ERA-40 data, *Journal of Climate*, 18, 7, 1032-1048.

Castellarin, A., Burn, D. H. and A. Brath (2008), Homogeneity testing : how homogeneous do heterogeneous cross-correlated regions seem ? *Journal of Hydrology*, 360, 67–76.

Coles, S. and M. Dixon (1999), Likelihood-Based Inference for Extreme Value Models, *Extremes*, 2, 1, 5–23.

Cooley, D., Cisewski, J., Erhardt, R. J., Jeon, S., Mannshardt, E., Omolo, B. O. and Y. Sun (2012), A survey of spatial extremes : Measuring spatial dependence and modeling spatial effects, *REVSTAT*, 10, 1.

Cunnane, C. (1988), Methods and merits of regional flood frequency analysis, *Journal of Hydrology*, 100, 1–3, 269–290.

Dales M. Y. and D. W. Reed (1989), *Regional flood and storm hazard assessment*, report No. 102, Institute of Hydrology, Wallingford, Oxon.

Darlymple, T. (1958), Flood frequency relations for gaged and ungaged streams, US Geological Survey.

Darlymple, T. (1960), Flood Frequency Analysis, 1543-A, US Geological Survey, *Water Supply Paper*.

Davison, A. C. and R. L. Smith (1990), Models for exceedances over high thresholds, *Journal of the Royal Statistical Society Series B (Methodological)*, 52, 3, 393–442.

Della-Marta, P. M. and J. G. Pinto (2009), Statistical uncertainty of changes in winter storms over the North Atlantic and Europe in an ensemble of transient climate simulations, *Geophysical Research Letters*, 36, L14703.

Della-Marta, P. M., Mathis, H., Frei, C., Liniger, M. A., Kleinn, J. and C. Appenzeller (2009), The return period of wind storms over Europe, *International Journal of Climatology*, 29, 437– 459.

Hjalimarsom, H. and B. Thomas (1992), New Look at Regional Flood Frequency Relations for Arid Lands, *J. Hydraul. Eng.*, 118, 6, 868–886.

Hosking, J. R. M. and J. R. Wallis (1988), The effect of intersite dependence on regional flood frequency analysis, *Water Resources Research*, 24, 4, 588-600.

Hosking, J. R. M. and J. R. Wallis (1993), Some statistics useful in regional frequency analysis, *Water Resources Research*, 29, 2, 271–281.

Hosking, J. R. M. and J. R. Wallis (1997), *Regional Frequency Analysis. An approach based on L-moments*, Cambridge, Cambridge University Press.

Kergadallan, X. (2013), *Analyse statistique des niveaux d'eau extrêmes - Environnements maritime et estuarien*, CETMEF, Centre d'études techniques maritimes et fluviales, Compiègne, 179p (in French).

Kjeldsen, T. R. and D. Rosbjerg (2002), Comparison of regional index flood estimation procedures based on the extreme value type I distribution, *Stochastic environmental research and risk assessment*, 16, 5, 358-373.

Laugel, A. (2013), *Sea state climatology in the North-East Atlantic Ocean: analysis of the present climate and future evolutions under climate change scenarios by means of dynamical and statistical downscaling methods*, Ph.D. Thesis, Saint-Venant Laboratory for Hydraulics, Université Paris-Est, Chatou, France.

Leckebusch, G. C., Renggli, D. and U. Ulbrich (2008), Development and application of an objective storm severity measure for the Northeast Atlantic region, M*eteorologische Zeitschrift*, 17, 5, 575-587.

Madsen, H. and D. Rosbjerg (1997), The partial duration series method in regional index-flood modeling, *Water Resources Research*, 33, 4, 737–746.

Madsen, H. and D. Rosbjerg (1998), A regional Bayesian method for estimation of extreme streamflow droughts, *Statistical and Bayesian methods in hydrological sciences*, UNESCO, Paris, 327-340.

Madsen, H., Rasmussen, P. F. and D. Rosbjerg (1997a), Comparison of annual maximum series and partial duration series methods for modeling extreme hydrologic events: 1. At-site modeling, *Water Resources Research*, 33, 4, 747-757.

Madsen, H., Pearson, C. P. and D. Rosbjerg (1997b), Comparison of annual maximum series and partial duration series methods for modeling extreme hydrologic events: 2. Regional modeling, *Water Resources Research*, 33, 4, 759-769.

Madsen, H., Mikkelsen, P. S., Rosbjerg, D. and P. Harremoës (2002), Regional estimation of rainfall intensity-duration-frequency curves using generalized least squares regression of partial duration series statistics, *Water Resources Research*, 38, 11, 21/1-21-11.

Mikkelsen, P. S., Madsen, H., Rosbjerg, D. and P. Harremoës (1996), Properties of extreme point rainfall III: Identification of spatial inter-site correlation structure, *Atmospheric Research*, 40, 77–98.

Pickands, J. (1975), Statistical Inference Using Extreme Order Statistics, *The Annals of Statistics*, 3, 1, 119-131.

Pinto, J. G., Karremann, M. K., Born, K., Della-Marta, P. M. and M. Klawa (2012), Loss potentials associated with European windstorms under future climate conditions, *Climate Research*, 54, 1–20.

Reed, D. W. (1994), *Rainfall frequency analysis for flood design*, in Coping with Floods, NATO ASI Series Volume 257, 59-75.

Renard, B. (2011), A bayesian hierarchical approach to regional frequency analysis, *Water Resources Research*, 47, W11513, 2011.

Renard B. and M. Lang (2007), Use of a gaussian copula for multivariate extreme value analysis : some case studies in hydrology, *Advances in Water Resources*, 30, 897–912.

Renggli, D., Leckebusch, G. C., Ulbrich U., Gleixner, S. N. and E. Faust (2011), The Skill of Seasonal Ensemble Prediction Systems to Forecast Wintertime Windstorm Frequency over the North Atlantic and Europe. *Monthly Weather Review*, 139, 3052–3068.

Ribatet, M. (2007), POT: Modelling Peaks Over a Threshold, *R News*, 7, 3.

Rosbjerg, D. (1985), Estimation in partial duration series with independent and dependent peak values, *Journal of Hydrology*, 76, 183-195.

Rosbjerg, D. and H. Madsen (1996), The role of regional information in estimation of extreme point rainfalls, *Atmospheric Research*, 42, 1-4, 113-122.

Roth, M., T. Buishand A., Jongbloed, G., Klein Tank, A. M. G. and J. H. van Zanten (2012), A regional peaks-over-threshold model in a nonstationary climate, *Water Resources Research*, 48, W11533.

Saha, S., Moorthi, S., Pan, H.-L., Wu, X., Wang, J., Nadiga, S., Tripp, P., Kistler, R., Woollen, J., Behringer, D., Liu, H., Stokes, D., Grumbine, R., Gayno, G., Wang, J., Hou, Y.-T., Chuang, H.-Y., Juang, H.-M. H., Sela, J., Iredell, M., Treadon, R., Kleist, D., van Delst, P., Keyser, D., Derber, J., Ek, M., Meng, J., Wei, H., Yang, R., Lord, S., van den Dool, H., Kumar, A., Wang, W., Long, C., Chelliah, M., Xue, Y., Huang, B., Schemm, J.-K., Ebisuzaki, W., Lin, R., Xie, P., Chen, M., Zhou, S., Higgins, W., Zou, C.-Z., Liu, Q., Chen, Y., Cucurull, L., Reynolds, R. W., Rutledge, G. and M. Goldberg (2010), The NCEP Climate Forecast System Reanalysis, *Bulletin of the American Meteorological Society*, 91, 1015–1057.

Scholz, F. W. and M. A. Stephens (1987), K-sample Anderson-Darling Tests, *Journal of the American Statistical Association*, 82, 399, 918–924.

Smith, R. L. (1990), Regional estimation from spatially dependent data, *unpublished*.

Stedinger, J. R. (1983), Estimating a regional flood frequency distribution, *Water Resources Research*, 19, 2, 503–510.

Stewart, E. J., Reed, D. W., Faulkner, D. S. and N. S. Reynard (1999), The FORGEX method of rainfall growth estimation - I: Review of requirement, *Hydrology and Earth System Sciences*, 3, 187-195.

Weiss, J., Bernardara, P. and M. Benoit (2014), Formation of homogeneous regions for regional frequency analysis of extreme significant wave heights, submitted to *Journal of Geophysical Research*.

7 Table captions

Table 1. Measures of regional dependence for each region (with the number of sites N indicated between parentheses): λ_r is the mean annual number of storms in the region, Φ is the adimensional function of regional dependence, $\beta_s(1)$ is the mean number of impacted

sites during a storm, 100_r is the regional return period (in years) of the storm causing at least one local 100-year event (equation (12) with T = 100) and D_{eff} is the regional effective duration (in years, along with the 95% confidence interval).

Table 2. Parameters of the regional distribution: γ (GPD scale parameter), k (GPD shape parameter), $y_{0.99}$ (100-year regional return level).

Table 3. Return periods (in years) of the storms with the highest normalized intensity observed in each region: $\tilde{T}_{s,loc}$, $\bar{T}_{s,loc}$, $\tilde{T}_{s,reg}$ and $\bar{T}_{s,reg}$ are respectively the empirical local return period, the theoretical local return period, the empirical regional return period and the theoretical regional return period.

8 Figure captions

Figure 1. Location of the 1847 sites extracted from the oceanic mesh of the ANEMOC-2 sea-state database.

Figure 2. Footprints of the storms of a) 15-18 February 1986, b) 11-13 December 1990 and c) 23-24 January 2009 (Klaus), where red dots indicate the impacted sites.

Figure 3. Map of threshold values of H_s exceeded on average once per year (m).

Figure 4. Division into six homogeneous regions.

Figure 5. Regional return period T_r against the local return period T for each region, as defined in equation (12). Curves for regions 3 and 4 are superimposed.

Figure 6. Return level plots of the regional distributions (crosses represent observations from each regional sample), together with the 95% confidence intervals obtained by bootstrap.

Figure 7. Map of estimated 100-year H_s (m).

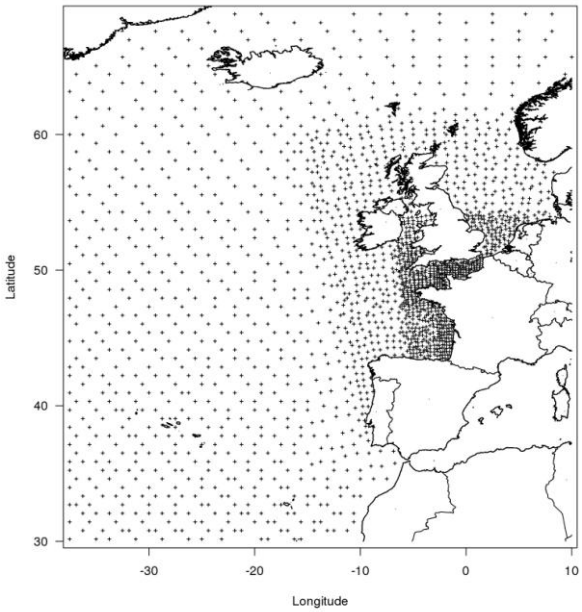

Figure 1. Location of the 1847 sites extracted from the oceanic mesh of the ANEMOC-2 sea-state database.

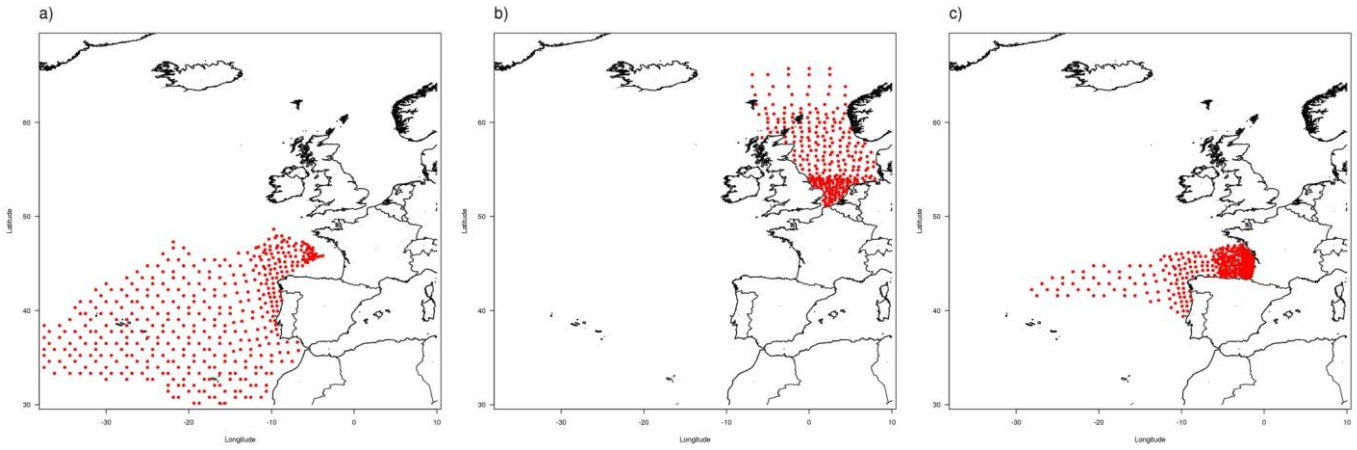

Figure 2. Footprints of the storms of a) 15-18 February 1986, b) 11-13 December 1990 and c) 23-24 January 2009 (Klaus), where red dots indicate the impacted sites.

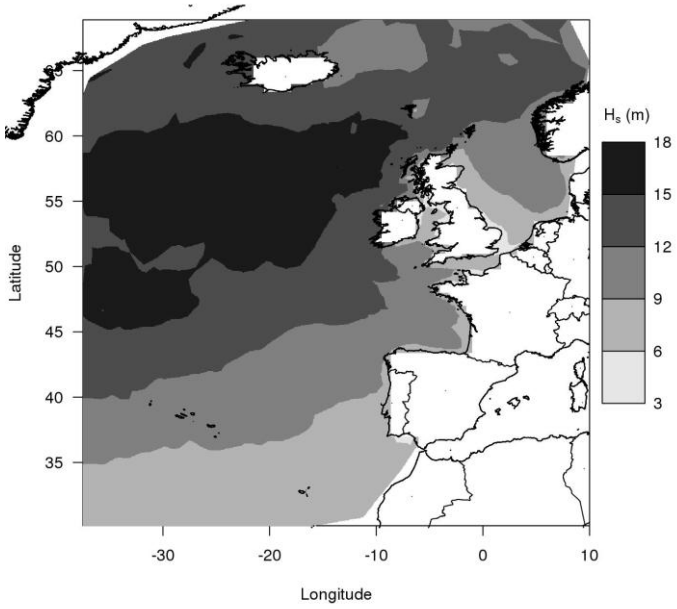

Figure 3. Map of threshold values of H_s exceeded on average once per year (m).

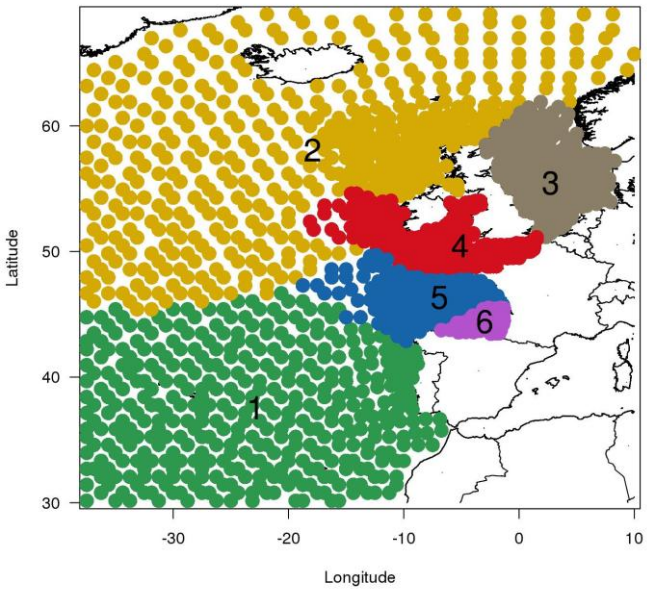

Figure 4. Division into six homogeneous regions.

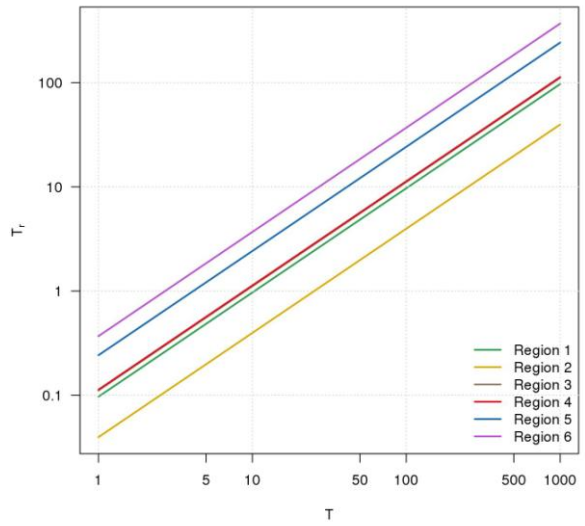

Figure 5. Regional return period T_r against the local return period T for each region, as defined in equation (12). Curves for regions 3 and 4 are superimposed.

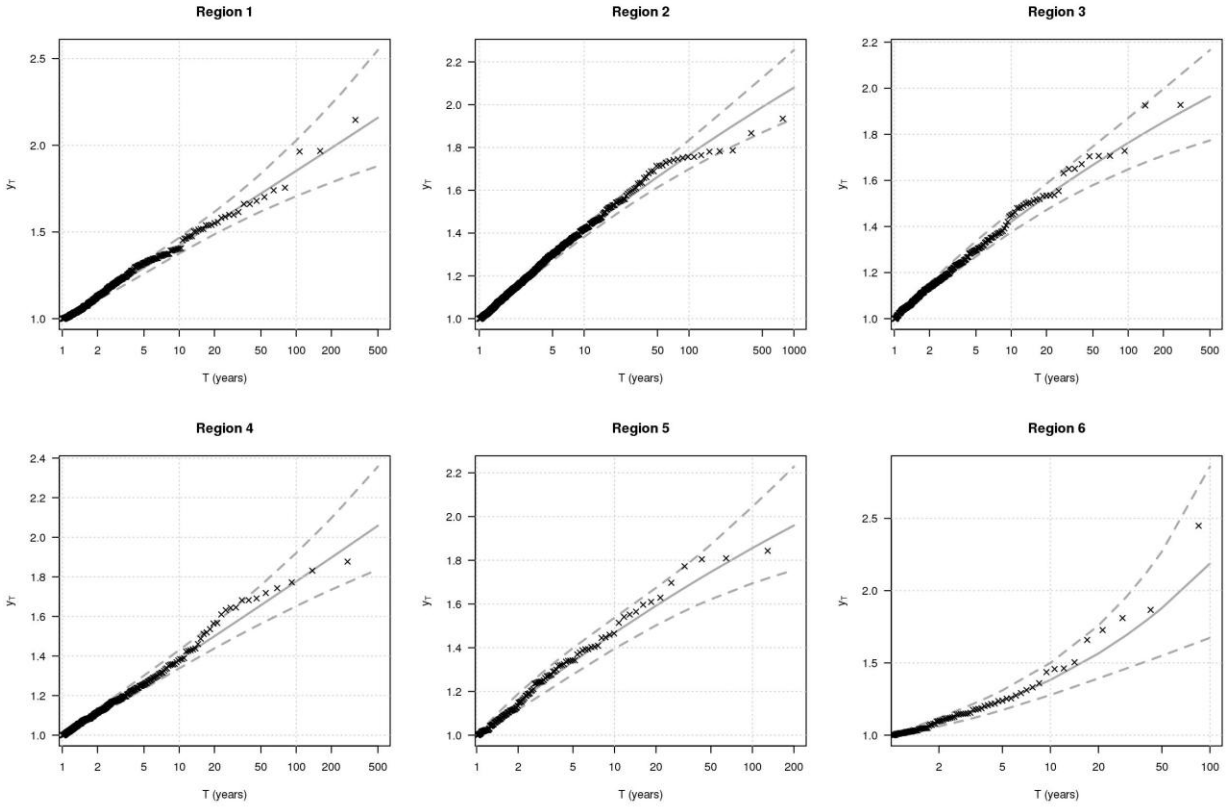

Figure 6. Return level plots of the regional distributions (crosses represent observations from each regional sample), together with the 95% confidence intervals obtained by bootstrap.

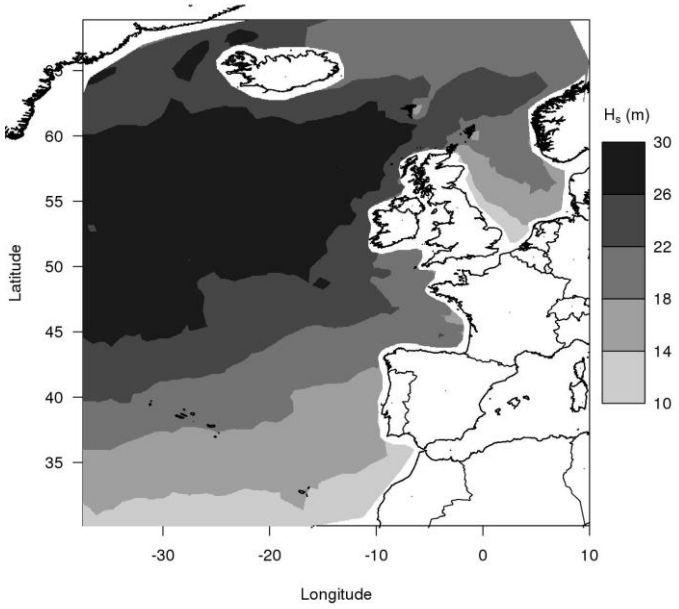

Figure 7. Map of estimated 100-year H_s (m).